

# DONuT (DRONE WITH ORIENTED THRUST)

(Aerodynamic Optimization of the DONuT rotor)

Marion MARDUEL

Alfonso VELENCOSO GOMEZ

Director of the projet: Sébastien PROTHIN

**Abstract**—The present work analyses designs of coaxial rotor systems in an attempt to maximize its performance in hover flight. The study is carried out with the software XROTOR and CROTOR. Influence of parameters such as tip radius, revolutions per minute (RPM),  $C_i$  and number of blades have been studied. The optimization process has been carried out on two possible models of the drone DONuT. Both of them are designed to allow for torque cancellation. In order to validate the designs, the optimized models have been 3-D printed to be tested in a test bench.

## I. CONTEXT

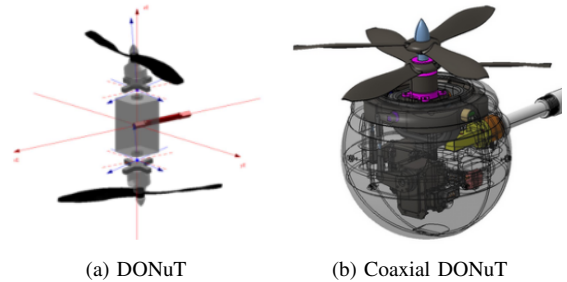
UAVs (Unmanned Air Vehicles) have been a main subject of investigations during the last decades. Civil UAVs have been studied as much as military ones. They are specially interesting due to their capability to carry out dangerous missions or even impossible ones with another kind of air vehicles. The development of smaller, lighter and more agile micro air vehicles is principally focused on fixed, rotary and flapping wing vehicles. Among the previous vehicles, the rotary wing ones are the best suited for reconnaissance or observation missions thanks to their high performance when hovering, which is the main flight mode of such missions. They have a structure similar to macro scale helicopters, therefore they are able to fly at quite high speeds, hover, and execute vertical take-off and landing (VTOL). It is the only configuration known to combine acceptable high and low speed characteristics including hovering. In addition, it is also the only controllable hovering object at the moment.

The ISAE Supaero's Aerodynamics and Propulsion Department (DAEP) is working on the design of a new micro aerial vehicle, the DONut (Drone with OriENted Thrust). This vehicle uses a counter rotating coaxial rotor that tilts in order to create drift forces and moments potentially usable for maneuverability. By doing so, the drone can be controlled without moving surfaces such as ailerons or rudders. This results in a smaller and more compact drone.

The tilting rotors allow the air vehicle to follow a desired trajectory while being robust against external perturbations such as wind gust. As said in [5], “the potential benefit from that kind of control is to get rid of any unnecessary control surface which would make the vehicle more sensitive to crosswinds”. Control laws that cancel external perturbations have been developed in previous projects of the DAEP (see [3]).

DONuT has been designed to carry out reconnaissance and observation missions. One of their possible future missions could be exploitation and exploration of caves on Mars.

There are two potential models. The DONuT has a tilting rotor above its center of gravity and the other one below it (fig 1a). The coaxial DONuT has both tilting rotors above its center of gravity (fig 1b). The DONuT has 6 degrees of freedom for each rotor, which enables the rotor to change its orientation even while hovering, while the coaxial DONuT has 6 degrees of freedom for both rotors therefore its orientation is fixed while hovering.



## II. PROBLEM STATEMENT

The rotors available in the market are mostly designed to be efficient when moving forwards and when hovering. However a single design can not be optimal in both configurations. As the drone DONuT will be operated mainly in hovering mode, the present paper aims at finding out the optimal geometry for this flight configuration. An optimization of the rotor geometry would increase the drone's autonomy, allowing it to perform longer missions.

Two possible models will be studied (fig 1a and fig 1b). The rotor must lift the drone weight. Therefore, the sum of upper rotor thrust  $T_U$  and lower rotor thrust  $T_L$  will be equal to the overall thrust  $T$  and to the drone's weight  $W$ .

$$T = T_U + T_L = W \quad (1)$$

Since the only control surfaces in this drone are the tilting rotor, the equilibrium can only be reached if they compensate each other's torque. The torque equation relates the upper rotor torque  $Q_U$  with the lower rotor torque  $Q_L$ :

$$Q_U + Q_L = 0 \quad (2)$$

### III. STATE OF THE ART

There are several theoretical aerodynamic approaches that can be followed to obtain the optimal geometry such as Simple Momentum theory, Blade Element Theory, Blade Element Momentum Theory (BEMT) or Free Vortex wake Method (FVM). The last one shows the best accuracy but needs a high computational cost. As seen in [7], BEMT shows good agreement with the FVM while being computationally five orders of magnitude faster.

An analysis using the BEMT for the second model of the DONuT was already carried out in [4]. However several simplifications were made, such as considering that the lower rotor did not disturb the flow passing through the upper rotor. Therefore this paper aims at conducting a new analysis with new tools: the free-software XROTOR and CROTOR.

#### XROTOR AND CROTOR

XROTOR is an interactive program for the design and analysis of ducted and free-tip propellers and windmills. Among their functions, there is the design of the minimum induced loss rotor (propeller or windmill) which has been the main tool to create our rotor designs. Some other functions have shown to be very useful. For instance, the interactive modification of a rotor geometry has allowed the geometry and rotor thickness to be changed in order to match the manufacturing constraints. For further details read [1].

CROTOR is a subroutine of XROTOR. It automates tedious procedures for designing or analyzing counter-rotating rotors in XROTOR while providing an effective user interface and reporting. It approximately models the effects of an upstream or downstream propeller and allows a system of coaxial rotors of minimum induced loss to be designed. For further details read [2].

Since the aerodynamic interference between upper and lower rotor is much stronger for model 2 than for model 1, it will be only considered for model 2. Therefore, model 1 will be designed with XROTOR and model 2 with CROTOR.

#### IV. EQUATIONS, OBJECTIVE FUNCTION AND PARAMETERS OF THE PROBLEM

This system's goal is to generate 5N of thrust while compensating for the torque. This amount of thrust can be obtained with an infinite number of designs. In this section, the design's parameters will be modified to study their influence. The objective is to find the best and most efficient design that still fulfills the imposed goals.

The addends of thrust equation (1) can be expressed as follows:

$$\begin{aligned} T_i &= Nb_i \int_0^{R_i} \frac{1}{2} \rho_\infty V_i^2 c_i (C_{li} \cos \gamma_i - C_{di} \sin \gamma_i) dr \\ &\simeq Nb_i \int_0^{R_i} \frac{1}{2} \rho_\infty (\Omega_i r)^2 c_i C_{li} dr \\ &= \frac{1}{2} Nb_i \rho_\infty \Omega_i^2 \int_0^{R_i} r^2 c_i C_{li} dr, \end{aligned} \quad (3)$$

With:

- $Nb_i$ . Number of blades of the rotor  $i$ .
- $C_{li}$ . Local lift per unit distance coefficient of the rotor  $i$ . It is related to the blade twist angle  $\beta_i(r)$ .
- $C_{di}$ . Local drag per unit distance coefficient of the rotor  $i$ . It is related to the blade twist angle  $\beta(r)$ .
- $\rho_\infty$ . Flow density of the upstream flow.
- $\Omega_i$ . Angular velocity of the rotor  $i$ .
- $c_i$ . Chord distribution of the rotor  $i$ .
- $R_i$ . Tip radius of the rotor  $i$ .
- $\gamma_i$ . Pitch angle of the rotor  $i$ . Simplifications have been done considering  $\gamma_i \leq 1$  and  $C_d \leq Cl$ .

The addends of torque equation (1) can be expressed as follows:

$$\begin{aligned} Q_i &= Nb_i \int_0^{R_i} \frac{1}{2} \rho_\infty V_i^2 c_i (C_{li} \sin \gamma_i + C_{di} \cos \gamma_i) r dr \\ &\simeq Nb_i \frac{1}{2} Nb_i \rho_\infty \Omega_i^2 \int_0^{R_i} r^3 c_i (C_{li} \gamma_i + C_{di}) dr, \end{aligned} \quad (4)$$

The value of  $\gamma$  can be obtained once the field of induced velocities is calculated.  $\rho_\infty$  depends on the upstream flow. The objective function that the present study looks to maximize is the Power Loading.

$$\begin{aligned} PL &= \frac{W}{P} \\ &= \frac{T_U + T_L}{|Q_U| \Omega_U + |Q_L| \Omega_L} \end{aligned} \quad (5)$$

With:

- $W$ . Drone's weight.
- $P$ . Power consumed in the generation of thrust.

It is a measure of efficiency of the system as it measures the amount of power consumed to generate a given amount of thrust, the higher this value is, the more efficient the system is.

Eventually, there are 5 parameters that can be modified during the optimization process:  $Nb$ ,  $C_l(r)$ ,  $\Omega_i$ ,  $c(r)$  and  $R$ . XROTOR and CROTOR calculates the optimal rotor geometry (chord and angle of twist along the blade) when providing as an input:  $Nb$ ,  $C_l(r)$ ,  $\Omega_i$  and  $R$ . These 4 parameters are the ones which are modified in the parametric study. Unfortunately, the inter-rotor distance can not be introduced as an input to CROTOR for the coaxial DONuT. Therefore, it optimizes a coaxial rotor geometry for a distance that cannot be modified and which probably is the distance needed to let the upper rotor's vena contracta fully develop.

## V. CHOICES OF DESIGN

With the aim of obtaining the optimal rotor design, a few choices have been made concerning some parameters.

### A. Fluid properties

As the prototype will be tested on the ground and DONuT missions will typically take place at low altitudes, the fluid properties set for the optimization are the  $ISA + 0^\circ C$  at sea level.

### B. Number of Blades

Since the resonance vibration is reduced with an odd number of blades, it had to be either 3 or 5 for each rotor, as more than 5 would be too many. The configurations studied are the following ones: 5-5, 3-3, 5-3 and 3-5. The first digit represents the number of blades of the upper rotor while the second one, the number of blades of the lower rotor. XROTOR and CROTOR show that the efficiency of all these configurations remains the same regardless of the number of blades.

### C. Airfoil

A complete optimization of the rotor should be carried out with an airfoil shape variation along the blade length. However, the same airfoil shape will be used in order to simplify the process. It is an airfoil with a relative thickness of 0.04 and a curvature of 0.06 (Fig 1).

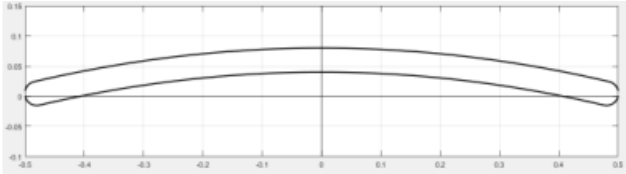


Fig. 1. Airfoil. Relative thickness: 0.04 - Curvature:0.06.

It is the same one used in the rotor optimization in [4] because it has shown good results at low Reynolds number, which will be the flight envelope for which the DONuT is developed.

The aerodynamic inputs for both XROTOR and CROTOR are synthesized in the Table I. Those inputs were determined from the polar curves issued from [6].

Parameter	Value
$Cl_0$	-1.98
$dCl/d\alpha$	10.5
$dCl/d\alpha$ @stall	0.1
$Cl_{max}$	1.06
$Cl_{min}$	-0.15
$Cd_{min}$	0.0450
$Cl(Cd_{min})$	0.542
$dCd/d(Cl^2)$	0.0397
$Re_{ref}$	100 000

TABLE I  
AERODYNAMIC INPUTS CONCERNING THE AIRFOIL FOR XROTOR AND CROTOR

Regarding the aerodynamic, the polar curves of the airfoil show that the  $C_l^{Stall}$  is around 1 and that the greatest  $C_l/C_d$  ratio occurs when  $C_l = 0.9$ . Therefore, the optimal design would have  $C_l$  around 0.9 without reaching  $C_l = 1.06$ . Indeed if this happens some sections of the blades would stall. The result would be a collapse in aerodynamic performance and insufficient rotor thrust. Since XROTOR uses a potential method for its calculation with several simplifications, the design has been done with values of  $Cl$  that do not exceed 0.7 to prevent the flow from stalling.

## VI. DONuT DESIGN

If XROTOR is to compile in order to design the rotor, some parameters must be entered. Those parameters must be determined to match constraints of performance and feasibility.

### A. XROTOR Configuration

The whole design of the rotor was conducted with XROTOR so that 30 sections were initialized all along the blades. Furthermore the computation is stopped if the number of iterations before obtaining the convergence of the calculations overtakes 40. The formulation used was the Betz-Prandtl distribution or Graded-Momentum Formulation which is computationally economical and well adapted for cases with advance ratio inferior to 0.5. At the end of the design of the rotor we obtained an advance ratio equal to 0.0005 so the use of this method is justified.

### B. Torque Cancellation

In the case of the DONuT where both rotors are separated by the fuselage of the drone, upper and lower rotors will have the same design. They will turn at the same number of revolutions per minute but in opposite directions. This asserts that both upper and lower rotors must provide 2.5N to respect the equation of Thrust 1 by delivering a global thrust of 5N. This also insures that the global resultant torque around the vertical axis is null which is necessary to allow the control of the DONuT during its flight.

### C. Geometrical Inputs

Among the required parameters for the use of XROTOR there are geometrical inputs. A few of them are still imposed by the work of a previous team like [3] on the DONuT. Indeed the  $R_T$  or tip radius is fixed at 125 mm while the hub radius  $R_H$  is equal to 20 mm. As seen in the previous Subsection VI-B the value of the thrust delivered by both upper and lower rotors must reach 2.5N. Additionally XROTOR imposes a constant lift coefficient all along the blades which has been chosen equal to 0.7 in compliance with V to avoid a stall in a section of the blades.

Again two other geometrical inputs must be defined: the number of blades  $N$  and the number of revolutions per minute (RPM) that will be imposed on the motor. A parametric study was conducted in order to fix their respective values.

1) *Parametric study:* Since the upper and lower rotors have the same design for the DONuT only two configurations of blades are relevant to study : 3-3 and 5-5. Additionally the number of RPM must stay in the envelope of use of the motor which is: [3000-8000] rpm. Considering those elements the efficiency, distribution of the Reynolds along the blades or load of the cases summarized in the Table II were examined.

	3-3	5-5
3000 rpm	case 1	case 2
4000 rpm	case 3	case 4
5000 rpm	case 5	case 6
6000 rpm	case 7	case 8
8000 rpm	case 9	case 10

TABLE II  
CONFIGURATIONS DEVELOPED

Experiments with XROTOR show that the distribution of propulsive efficiency along the blades stays the same if the number of blades N or the number of RPM are changing.

However as shown on the graph Figure 2 the power loading defined previously (5) regularly decreases when the number of RPM increases and the decline of the PL due to the reduction of the number of blades is negligible.

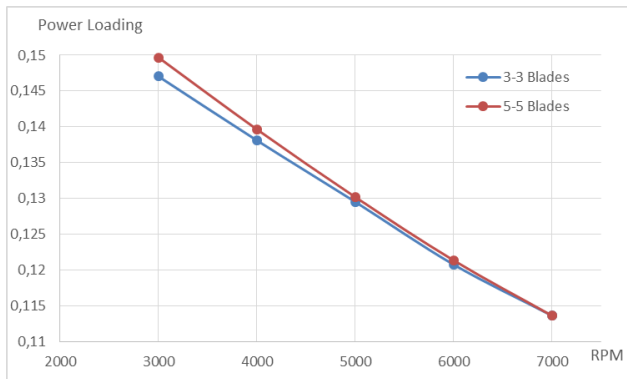


Fig. 2. Evolution of the Power Loading for different configurations

Since the PL is the objective function to be maximized in order to obtain an efficient rotor it is relevant to focus on low number of revolutions per minute like 3000 or 4000 rpm.

Alongside the study of the evolution of the power loading the distribution of the Reynolds all along the blades for the different cases of the Table II was calculated. The graph Figure 3 clearly shows that when the number of RPM increases the Reynolds number as for it decreases. Considering that the previously presented airfoil 1 is suitable at low Reynolds it is relevant to focus on a configuration which tends to have reasonable values of Reynolds. This means 7000, 6000, 5000 or potentially 4000 rpm for the studied cases.

A concession has to be made in order to match the two previous observations: match an adapted airfoil and a sufficient efficiency. Consequently the most appropriated configuration

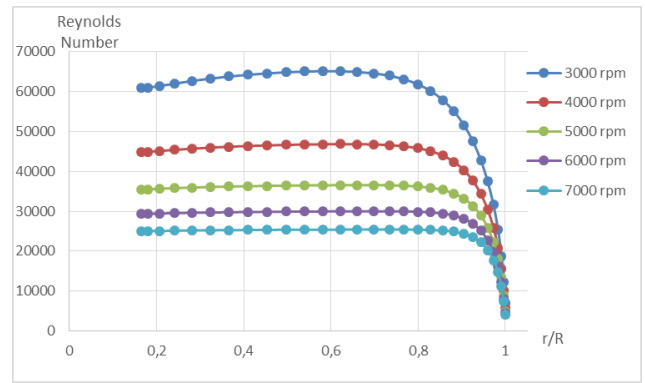


Fig. 3. Evolution of the Reynolds number along the blades for different RPM

for the DONuT seems to be the one at 4000 RPM.

Now we will focus on the influence of the number of blades in order to choose the best configuration between the 3-3 layout and the 5-5 option.

As seen on the graph Figure 2 the number of blades does not truly improve the power loading. However the graph Figure 4 highlights an interesting influence of N. The graph represents the thickness all along the blades of the rotor for both cases (3-3 configuration and 5-5 layout). The rise from 3 to 5 blades leads to a global decline of the thickness in every section of the blades. This observation leads to the adoption of the 3-3 layout because of fabrication constraints imposing a thickness superior than 0.5 mm in every part of the rotor. If this constraint is not respected the final rotor could not be printed with the 3D printing technologies from the DMSM at ISAE-Supaero. To sum up the lower rotor will have 3 blades turning at 4000 rpm while the upper one will turn at -4000 rpm with 3 blades.

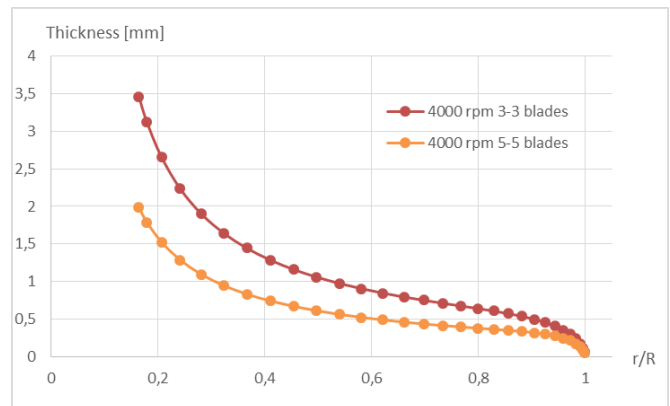


Fig. 4. Evolution of the thickness along the blades for 2 configurations (3-3 layout & 5-5 option) at 4000 rpm

2) *Basic Configuration for optimization:* At the end of the parametric study, VI-C1 all the geometrical inputs for XROTOR are defined. They are all summarized in the Table III and the design of the rotor can start.

Parameter	Value
Number of Blades N	3
Tip Radius $R_T$ [m]	0.125
Hub Radius $R_H$ [m]	0.02
RPM [rpm]	4000
Thrust[N]	2.5
Lift Coefficient along the airfoil $C_L$	0.7

TABLE III  
INPUT PARAMETERS

#### D. Design Process

Thanks to the aerodynamic and geometrical inputs from Tables I and III XROTOR can optimize a chord law and a twist law in order to obtain a rotor with a minimum induced loss. The process to obtain this design is sketched in the Figure 5.

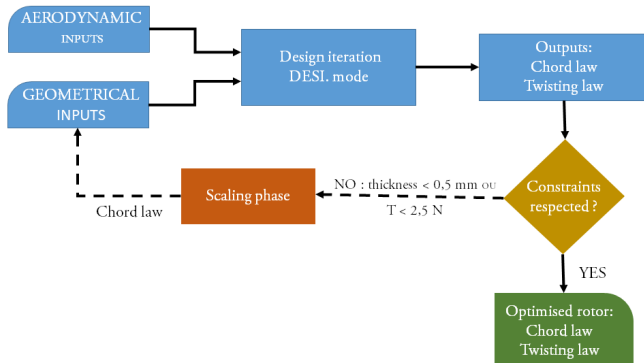


Fig. 5. Iterative process on XROTOR

The first step in the design process consists of entering all the geometrical and aerodynamic inputs. Then a first iteration is compiled with XROTOR in the DESI. mode which gives two outputs : a chord law and the twist that must be imposed to the rotor to enable it to provide 2.5N. As soon as these outputs are obtained it is possible to trace the evolution of the thickness along the Blades in order to check that the design purposed by XROTOR matches with the constraints of feasibility. If the thrust delivered is superior or equal to 2.5 N and if every section has a thickness superior or equal to 0.5 mm the design is approved. Otherwise manipulations are necessary to reach the final version of the design with the minimum induced loss of the rotor.

1) *First Iteration:* As drawn Figure 4 the first iteration with XROTOR systematically gives a design too fine in some sections of the blades. Consequently the design is achieved with a tip radius of 135 mm and a requested thrust of 2.7N instead of 125 mm and 2.5N. Then a new iteration is completed based on those new inputs.

2) *Final Design:* Once the new iteration is completed only sections in the range of  $0 < r < 125$  millimeters will be take into account. The thrust provided still reach 2.5N despite the fact that some sections are ruled out because as seen on the graph 6 which presents the distribution of the propulsive

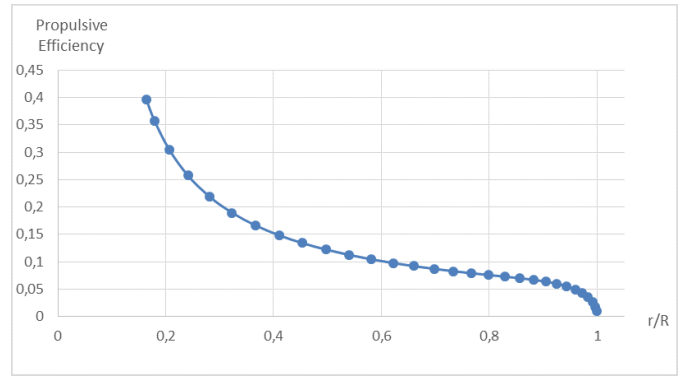


Fig. 6. Distribution of the propulsive efficiency along the blade. Input Parameters : 3-3 configuration, 4000rpm, Tip radius 125mm, Hub Radius 20mm, Cl 0.7, Thrust 2.5N.

efficiency all along the blades the last sections are not really efficient. Efficiency suddenly drops around 95% of the radius and this corresponds with a collapse on the same abscissa on the traction curve.

It seems that thickness has been improved but is still inadequate to fit with constraints of fabrication.

That is why an operation of scaling is imposed to the chord law all along the blades according to the following equation :

$$Chord_{new} = Chord_{old} * (A + B * \frac{r}{R}) \quad (6)$$

where :

- A = 1
- B = 0.285

The value of B was determined so that the chord on the abscissa of 125 mm from the center of the rotor implies a thickness of 0.5 mm on the same abscissa. If we apply the scaling law described with the equation 6 to the thickness, knowing that the latter is equal to 4% of the chord, it imposes :

$$\begin{aligned} B &= \left( \frac{0.5[mm]}{thickness(12.5cm)[mm]} - 1 \right) * \frac{R}{12.5[cm]} \\ &= \left( \frac{0.5}{0.436} - 1 \right) * \frac{13.5}{12.5} \\ &= 0.285 \end{aligned} \quad (7)$$

This modification of the chord law induces alterations of the thrust provided by the rotor. This is why a twist update step is performed with XROTOR's OPTI. mode in order to obtain the final optimized design.

The Figure 7 shows different chord laws. It represents the evolution of the chord for a basic design and the final one. The basic design is the one obtained just before the scaling step of the chord law previously explained. The final one is the design got at the end of the whole process.

The twist corresponding to this final design is represented on the graph on the Figure 8. Its value monotonically decreases from 36.89° at the hub to 6.32° at the blade tip.

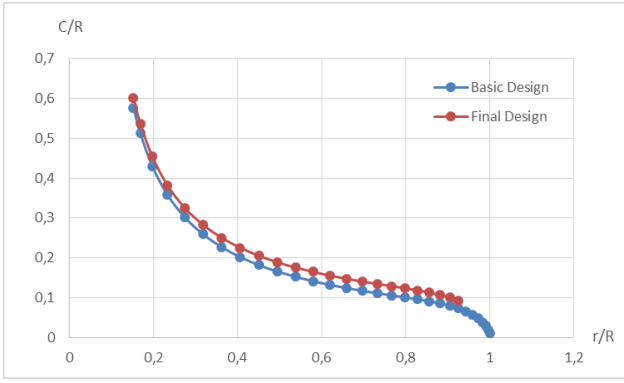


Fig. 7. Distribution of the chord for two cases. Firstly with the design before the scaling step. Secondly with the final design at the end of the process. For both cases  $r/R = 1$  if  $r = 135$  mm

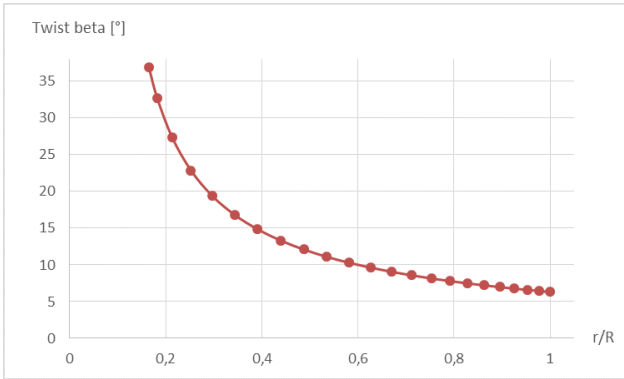


Fig. 8. Evolution of the twist [°] along the blades.  $R_t = 125$  mm .

## VII. COAXIAL DONUT DESIGN

In order to obtain an efficient and feasible design, a parametric study and further modifications to match fabrication constraints have been conducted.

### A. Torque cancellation

Torque cancellation is obtained by satisfying the torque equation (2). CROTOR does not allow the torque generation of each rotor to be imposed but it is possible to choose their power consumption and RPM individually. Therefore, the procedure followed has been choosing the power supplied to each rotor as a function of its angular velocity to satisfy the torque compensation. Equation 2 can be expressed as follows:

$$\frac{P_U}{\Omega_U} + \frac{P_L}{\Omega_L} = 0, \quad (8)$$

Thanks to this, the study of different angular velocities between both rotors can be done while still satisfying the torque cancellation.

### B. Parametric study

The configuration chosen as a base for the study is the following one:

It is convenient to point out that with CROTOR the thrust generated can not be chosen at the beginning of the design

Parameter	Value
Number of blades	5
Tip radius [m]	0.15
Hub radius [m]	0.02
RPM	3500
Power[W]	40
Approximate $C_l(r)$	0.6

TABLE IV  
BASE CONFIGURATION

and it is obtained at the end as a result. Therefore, a power of 40W has been chosen for the study because it enables the following configurations to provide around 5N.

Hereafter, the influence of the different parameters is shown and commented.

1)  $C_l$ : The approximate value of  $C_l$  along the blade's length can be specified. Its influence on the objective function is shown in the Table V.

Approximate $C_l(r)$	PL [N/W]
0.5	0.115
0.6	0.12
0.65	0.125
0.8	0.1275

TABLE V  
BASE CONFIGURATION'S  $C_l$  MODIFICATION AND ITS INFLUENCE ON PL

As it was said in Section 1, its value should not be greater than 0.7. As the performance increases with  $C_l$ , the value chosen is 0.68.

2)  $RPM$ : The influence of angular velocity expressed as RPM (both rotors spinning at the same speed) is shown in the Table VI.

RPM	PL [N/W]
3000	0.125
3500	0.12
4000	0.1175
6000	0.1025

TABLE VI  
BASE CONFIGURATION'S RPM MODIFICATION AND ITS INFLUENCE ON PL

For these values, the PL increases when the RPM value decreases. As the minimal RPM value of the engines used by the prototype of the drone is around 2000, the minimal value for the study will be 3000.

Designs with rotors spinning at different angular velocity have been studied, however there was not any other configuration where the PL was greater than both rotors spinning at 3000 RPM. Therefore, this is the optimal velocity for both of them.

3)  $Radius$ : The optimized rotor radius had to be greater than 0.15 m because CROTOR could not converge into a solution for a lower number when spinning 3000 RPM. Designs with lower radius were obtained for higher values of RPM but they were much less efficient.

The influence of the tip radius of the rotor (both rotor having the same radius) is shown in the Table VII.

Radius [m]	PL [N/W]
0.15	0.12
0.2	0.1275
0.25	0.125
0.3	0.1225

TABLE VII

BASE CONFIGURATION'S RADIUS MODIFICATION AND ITS INFLUENCE ON PL

When both rotors have the same radius, the desired tip radius value is 0.20m.

The case when the tip radius value is not the same for upper rotor and lower rotor has been studied as well (Fig. 9).

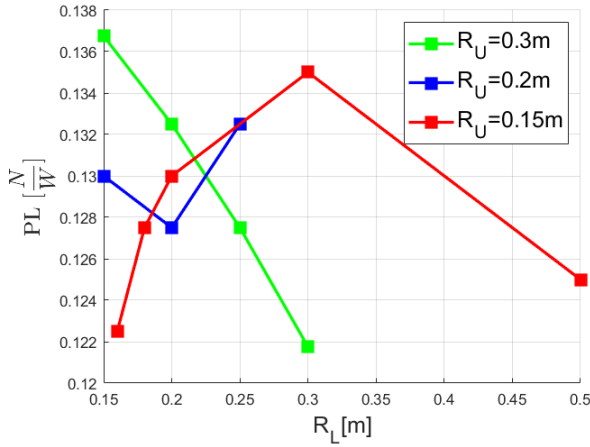


Fig. 9. Evolution of PL with  $R_U$  and  $R_L$

The Figure 9 shows that the optimal design has different values for the upper and lower rotor. It would have been interesting to see the evolution of the case  $R_U = 0.2m$  for greater values of  $R_L$  but CROTOR could not converge onto a solution for these cases. However, the chord and thickness in those cases are extremely low (below 1mm of chord and 0.04mm of thickness at 75% of the chord).

The most efficient configuration is obtained with  $R_U = 0.3m$  and  $R_L = 0.15m$ .

4) *Number of Blades*: As it was said in the Chapter V, the number of blades has not a significant influence on the PL. Therefore, from a aerodynamic point of view it makes no difference to have either  $Nb = 3$  or  $Nb = 5$ .

### C. Preliminary design

After this parametric study, we can conclude that the most efficient configuration should be close to the one shown in the Table VIII.

Its PL could not be obtained because CROTOR could not converge into a solution. However, it would be very interesting to have this value in order to confirm that it is actually the most efficient so far.

Parameter	Value
Number of Blades	3 or 5
Upper Tip Radius [m]	0.3
Lower Tip Radius [m]	0.15
Hub Radius [m]	0.02
RPM	3000
Approximate $C_l(r)$	0.68

TABLE VIII

DESIGN RESULTING FROM THE PARAMETRIC STUDY

### D. Fabrication constraints

The manufacturing method chosen for these rotors is 3D printing. It is a method with big advantages: it is cheap, it creates prototypes in just a few hours and 3D printers are available at the DMSM (Department of Structural and Material Mechanics) of ISAE-Supaero. However, it has some disadvantages that make impossible to obtain an design as the one showed in the Table VIII. These disadvantages are the constraints of minimal thickness (0.5mm) and maximum size (horizontal base of 254mm x 254mm).

As the relative thickness of the airfoil is 0.04, the minimum chord is  $0.5mm/0.04 = 12.5mm$ . The size constraint imposed by the 3D printer's horizontal plate implies that the maximum radius is 141mm with a 3 blades rotor and even lower for a 5 blades rotor.

### E. Feasible design

A design that satisfies the constraints could not be obtained with CROTOR as in all its optimization the chords decrease until zero at the tip. Therefore, the chord is usually below the minimum printable value after the 85% of the blade's length.

The procedure followed to obtain a feasible design as efficient as possible is the following one:

1) Creating a design with the same parameters that the one aimed but a radius 15% bigger and a generated thrust 20% (as shown in the Table IX). Since it is needed to have greater thickness and the 3-blade rotor proved to increase it (see Fig(Fig. 4), the number of blades chosen is 3. With CROTOR the optimization of this design is obtained (chord and twist angle laws).

Magnitude	Value
Number of Blades	3
Upper Tip Radius [m]	0.17
Lower Tip Radius [m]	0.17
Hub Radius [m]	0.02
RPM	3000
Approximate $C_l(r)$	0.68
Thrust generated	0.61
Resulting torque	0

TABLE IX

BASE DESIGN FOR THE FEASIBLE ONE

2) Its chord law has been increased with the Equation 6. With  $A=1$  and  $B=0.15$ , the new chord law satisfies the manufacturing constraint of thickness from  $r=0$  until  $r=141mm$ . The chord values at the beginning and at the end

of this step are shown in Fig. 10 and 11.

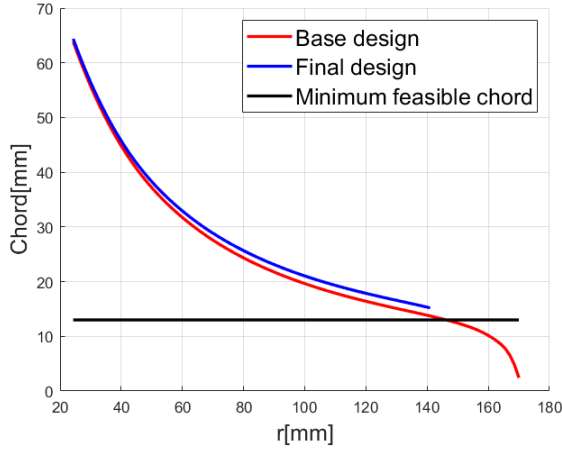


Fig. 10. Upper rotor. Process of increasing chords.

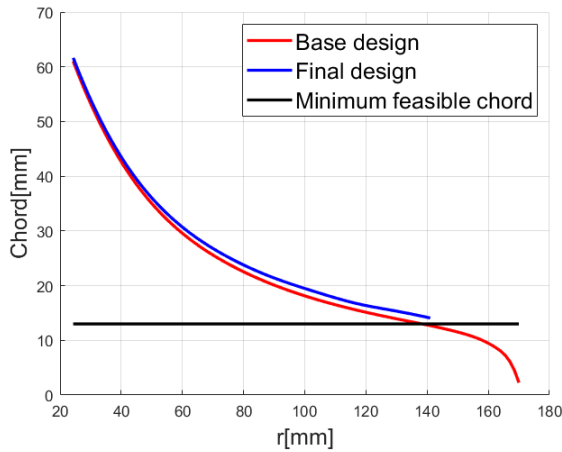


Fig. 11. Lower rotor. Process of increasing chords.

3) CROTOR calculates the new optimal torsion law for the modified design. As a result, its  $C_l(r)$  function is obtained.

4) The sum of contributions to the thrust of the upper and lower rotor's blade sections from  $r=0$  until  $r=141$ mm must be equal to 5N. Thrust is calculated as seen in the Equation 3. If the design does not match this requirement, the whole process restarts with a new value of power supplied.

Eventually, the final design is obtained. Its parameters and its chord and torsion angle laws are shown in the Table X and in the Figures 12 and 13.

### VIII. COMPARISON BETWEEN A PAIR OF COAXIAL ROTORS AND A SINGLE ROTOR.

It is of great interest to compare the performance of a coaxial rotor system with that of a single rotor according to

Parameter	Value
Number of Blades	3
Upper Tip Radius [m]	0.141
Lower Tip Radius [m]	0.141
Hub Radius [m]	0.02
RPM	3000
Approximate $C_l(r)$	0.6

TABLE X  
FEASIBLE DESIGN

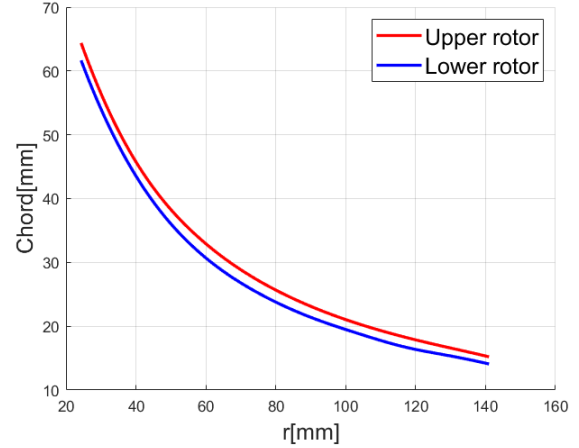


Fig. 12. Final design. Law of the chord.

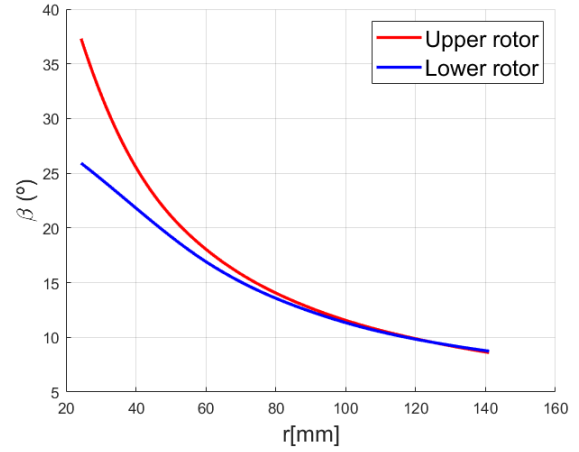


Fig. 13. Final design. Law of the torsion angle.

XROTOR and CROTOR. To do it properly, the coaxial rotor designs have been compared with two different single rotor designs: one with the same radius and another one with the same disc loading (see Fig. XI).

System	PL
Coaxial rotors (R=0.2m)	0.1275
Single rotor (R=0.2m)	0.1253
Single rotor (R=0.283m)	0.123

TABLE XI

COMPARISON BETWEEN COAXIAL ROTORS AND SINGLE ROTOR

These designs are calculated with the values of RPM,  $C_l$

and number of blades shown in the Table VI. All of them generates 5N of thrust.

According to this calculation, the performance of the coaxial configuration is the most efficient for this point of operation.

#### IX. 3D MODEL OF THE COAXIAL DONuT ROTOR, CADs AND 3D PRINTED MODELS

The CAD models have been done by PhD S. PROTHIN based on the chord and twist laws determined in the design phase (Fig. 14 and Fig. 15).

The 3-D printed models have been manufactured in the DMSM by M. GAGNEUX (Fig. 16, Fig. 17 and Fig. 18).

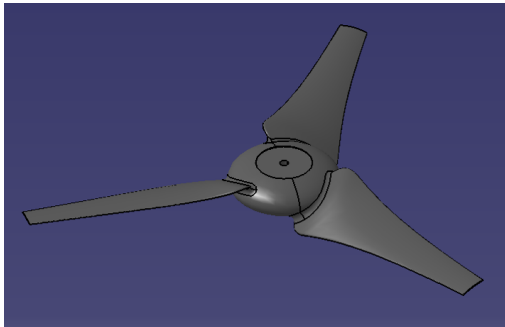


Fig. 14. Upper rotor - CAD

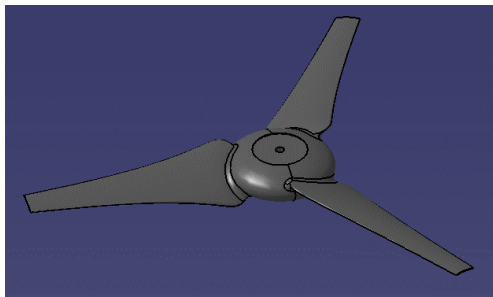


Fig. 15. Lower rotor - CAD



Fig. 16. Printed upper rotor



Fig. 17. Printed lower rotor



Fig. 18. Both printed rotors

#### X. COAXIAL DONuT ROTOR TEST

In the following days, the printed models will be tested in a test bench from the DAEP at ISAE-Supaero. They will be tested individually and later on together in a coaxial position. The thrust generated and power consumed by each rotor will be measured for a given RPM value. Their performance will be measured with the power loading value. If they show a good performance when providing 5N of thrust, these designs could be validated.

#### XI. COMPARISON DONuT - COAXIAL DONuT

The aim of this Section is to compare the different designs obtained thanks to XROTOR and respectively CROTOR at the end of the optimization step.

##### A. Comparison of the Chord Law

The Figure 19 illustrates the comparison of the chord laws of DONuT configuration (two identical rotors separated by the body of the drone) and the coaxial one. It appears that laws are roughly equivalent. They are all parabolic in shape and similarly decrease. There is no major difference to note.

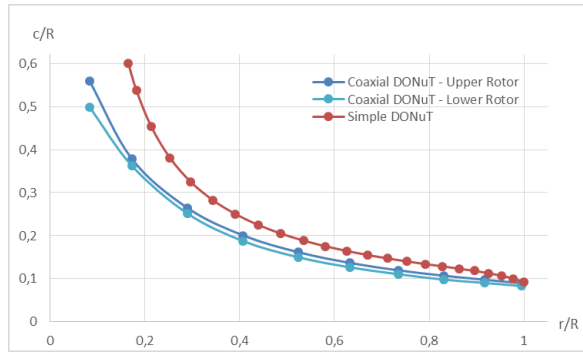


Fig. 19. Comparison of chord laws

### B. Comparison of the Twist Law

The Figure 20 allows to compare the twist laws got for the DONuT and the coaxial one. If laws for the upper rotor of the coaxial DONuT (in green) and the DONuT (in blue) are really similar, the law of the lower rotor (in orange) seems more linear.

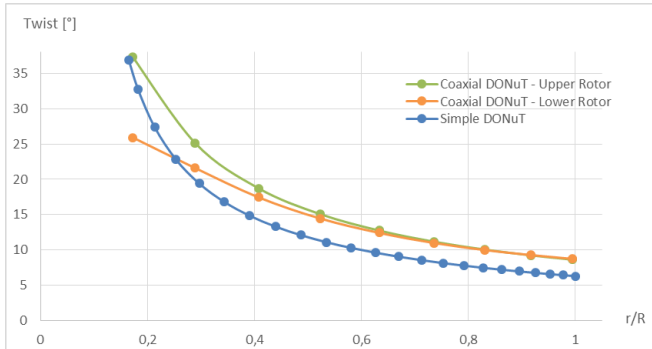


Fig. 20. Comparison of twist laws

## XII. CONCLUSIONS ABOUT THE DESIGN OF THE DONuT AND XROTOR.

1. XROTOR allows the user to adapt the method used for the computation. This point is really useful because we could use the Graded-Momentum Formulation which is very adapted for low advance ratios and operates with very little computational time.

2. The chord and twist laws obtained seem to be correct since XROTOR gave the same results using the Graded-Momentum formulation and the potential one. If differences appear on the performance between the theoretical efficiency or traction evolution and the experimental ones this could come from the input of airfoil data.

Indeed all the coefficients required as inputs in XROTOR were evaluated based on polar curves from [6]. Their calculation was sometimes a little bit complicated.

3. XROTOR does not allow to take into account the modification of the flow caused by the presence of the body of the drone. If perturbations of the flow are less significant than in the case of the coaxial DONuT the flux is all the same disturbed for the lower rotor.

4. Due to a lack of time we can not conduct experiments. However it is essential to carry out experimental measures in order to determine the exact power loading or efficiency of the rotor and to ascertain the traction curves of the blades. With this aim in mind it could be possible to conduct similar experiments than for the coaxial DONuT on test bench available from DAEP at ISAE-Supaero as explained on Section X. Such experiments are vital to validate the design obtained during this study.

5. The 3-3 and 5-5 blade configurations have shown the same power loading. Therefore, the design decision on the number of blades is not imposed by the aerodynamic. In this report, the number of blades used is 3-3 essentially regarding the manufacturing process.

6. To deal with this work in depth it could be relevant to study the loads endured by the blades when rotors are turning. This is normally enabled by XROTOR but needs additional information about the material of the rotors.

## XIII. CONCLUSIONS ABOUT THE COAXIAL DONuT'S ROTOR DESIGN AND CROTOR.

The following main observations and conclusions have been drawn from the present study:

1. CROTOR has proven to be a very useful tool as it allows for obtaining designs with very little computational time thanks to being based on a potential theory. This has enabled the creation of a big amount of different designs to complete a parametric study.

It enables the torque cancellation for any RPM value of upper and lower rotors since it is possible to introduce the power consumed and the angular velocity of each rotor.

2. CROTOR has as well some limitations:

Firstly, as it is based on a potential theory, there are several phenomena that it does not take into account. Therefore, its analysis and design would not match precisely the experimental measures in some cases.

Secondly, it does not have the inter-rotor distance as an input, therefore we assume that it calculates the optimal design for a distance large enough to let the upper rotor's vena contracta fully develop. In the cases where it is lower than this one, it is not possible to obtain a correct optimization. This is the case of our design. As this point is of big influence, in the future it will be necessary to find an optimization tool that allows for introducing the inter-rotor distance as an input in the optimization process.

Thirdly, it has shown convergence issues while optimizing a geometry for a rotor with a radius lower than 0.15m at 3000 RPM.

3. The 3-3, 3-5, 5-3 and 5-5 blade configurations have shown the same power loading. Therefore, the design decision on the number of blades is not imposed by the aerodynamic. In this report, the number of blades used is 3-3 regarding the manufacturing process.

4. Coaxial rotors is an interesting aerodynamic option according to CROTOR and XROTOR because an optimized coaxial rotor has higher PL than an optimized single rotor with the same radius tip, and higher PL than an optimized single rotor with the same disc loading.

5. The optimal configuration has different radius tip values for the upper rotor than for the lower one. In this study, the optimal values are 30 cm for the upper radius and 15 cm for the lower radius.

6. The extremely low values of thickness make the optimal design difficult to manufacture and to endure aerodynamics forces. Therefore, it should be convenient to search for new tools able to find optimal designs with higher chord values. Higher chord and thickness values are obtained with lower values of radius tip. However, CROTOR shows convergence problems for chord values lower than 15 cm.

7. The results shown in this report have been compared with the ones shown in [4], where the study was carried out with the BEMT approach. There is an agreement in the chord evolution form but a disagreement in the torsion angle evolution form. In both studies, the upper and lower laws of chord are very similar. However, the upper rotor torsion law has higher values than the ones of the lower rotor, while in [4] the opposite effect is shown. Another difference is that in this study the torsion law values are roughly 3 times the ones of the BEMT study.

8. The laws of chord and torsion angle obtained in this study can be explained as follows: resultant velocities are higher at the lower rotor than at the upper rotor because it is operating in a slipstream with both axial and tangential components. As a consequence, given similar lift coefficients, an optimized lower rotor will have a slightly smaller chord and less twist.

#### ACKNOWLEDGMENTS

At the end of this paper we want to thank our tutor M. PROTHIN for his help all along the project. His aid was compulsory to generate CATIA visualizations from the chord and twist laws obtained and to begin experiments with the coaxial DONuT. We also thank M. LAGHA for explaining us the basics of XROTOR, M. GAGNEUX for printing the

rotors for the coaxial DONuT and M. JARDIN for his BEMT software and his guidance when using it.

#### REFERENCES

- [1] DRELA M. Xrotor user guide. 2003.
- [2] CARTER P. Subroutine crotor user guide. 2011.
- [3] DEFAY F. RAYNAUD G. Prothin, S. and LAMBERT L. Drone with oriented thrust (donut). 2014.
- [4] Hadengue F. Prothin, S. and Laroche de Roussane E. Optimisation d'un rotor contrarotatif pour drone. 2017.
- [5] RAYNAUD G. PROTHIN S., DEFAY F. and LAMBERT L. A vectoring thrust coaxial rotor for micro air vehicle: Modeling, design and analysis. 2013.
- [6] PROTHIN S. Donnée aéro camberplate ep4c6 - excel.
- [7] M. Syal and J. Gordon Leishman. Contributions to the aerodynamic optimization of a coaxial rotor system. 2008.